

Supporting information

Nonlayered 2D ultrathin molybdenum nitride through the ammonolysis of molybdenum dioxide

Yuqiao Wang,^{a,c} Chuanyong Jian,^{a,b} Wenting Hong ^{a,b} and Wei Liu ^{a,c*}

^a CAS Key Laboratory of Design and Assembly of Functional Nanostructures, Fujian Provincial Key Laboratory of Nanomaterials, Fujian Institute of Research on the Structure of Matter, Chinese Academy of Sciences, Fuzhou, 350002, China.

^b University of Chinese Academy of Sciences, Beijing, 100049, China.

^c Fujian Science & Technology Innovation Laboratory for Optoelectronic Information of China, Fuzhou 350108, China

E-mail: liuw@fjirsm.ac.cn

Contents

1. Material and methods

2. Figures

3. Tables

References

1. Material and methods

The synthesis of 2D MoN flakes involves a two-step process. First ultrathin 2D MoO₂ flakes were directly grown on the SiO₂/Si substrate from the thermal reduction of MoO₃. Then, using urea as the nitrogen source, the isolated MoO₂ flakes were nitrated via an ammonolysis reaction.

1.1 Growth process of the 2D MoO₂ flakes

2D MoO₂ flakes were grown in a CVD system at atmospheric pressure. A porcelain boat with 20 mg MoO₃ powders (99.99%) was placed in the center of the tube furnace, and the 260 nm SiO₂/Si substrate was placed face down above MoO₃ powders. The furnace was flushed with high purity Ar to remove oxygen. Then, the furnace was heated to growing temperature (790, 810 or 830 °C) within 80 min and kept at this temperature for 5 min under 100 sccm Ar carrier flow. After the growth, the system was allowed to naturally cool down to room temperature.

1.2 Transformation of 2D MoO₂ to 2D MoN flakes via ammonolysis

The MoO₂ flakes were transformed to MoN flakes using an ammonolysis reaction under the Ar gas flow. Urea particles were used as a source gas for the flow of NH₃. The MoO₂ samples were placed at the center of the tube furnace. The quartz tube was purged with ultrahigh-purity Ar gas. Then, the furnace was heated up to 700 °C at a heating rate of 5 °C/min under 80 sccm Ar gas. The total duration for the reaction process was 80 min after the temperature of the system had reached 700 °C. After the ammonolysis, the samples were naturally cooled to room temperature.

1.3 Electrochemical Measurements of the MoN

An electrochemical microreactor with three electrodes was fabricated in our system. Ag/AgCl and pencil graphite were used as the reference electrode and counter electrode, respectively. The remaining electrode were connected to the MoN to monitor the catalytic signal. Polarization curves were measured in a H₂SO₄ (0.5 M) or KOH (1.0 M) droplet on the CHI 660E electrochemical station. The scan rate is 2 mV

s^{-1} . All measurements were without iR compensation. In all measurements, only the exposed windows of the MoN flakes contribute to the HER activity.

1.4 Characterization

OM images were taken with an ECLIPSE LV150N, Nikon instrument, and the AFM images were performed with a Dimension ICON. The TEM analysis were carried out using TF20, Jeol 2100F. The XPS analysis were carried out in an ESCALAB 250Xi.

1.5 Device Fabrication and measurement

The MoN flakes were transferred onto a SiO_2/Si substrate with PMMA assistance. The devices were fabricated by e-beam lithography (EBL) and evaporation system with metal electrodes pairs of Ti/Au (10/50 nm). Electrical properties were performed with a semiconductor parameter analyzer.

1.6 Calculation Details

DFT calculations have been carried out with Vienna Ab initio Simulation Package (VASP). The calculations are based on the Perdew-Burke-Ernzerhof (PBE) exchange-correlation functional within the generalized gradient approximation (GGA). The energy cutoff is 400 eV and first order Methfessel-Paxton smearing is used with a width of 0.2 eV. The Normal algorithm controls the self-consistent iterations with 10^{-5} eV tolerance and 100 maximum steps. The structures are optimized to a maximum force of 0.02 eV/Å. The k-spacing is $7 \times 7 \times 6$ mesh for the calculation of geometry optimization and density of states. The reciprocal space integrations are carried out at the gamma-points. The electronic structure of the bandstructure and density of states reveals the metallic property for MoN.

2. Figures

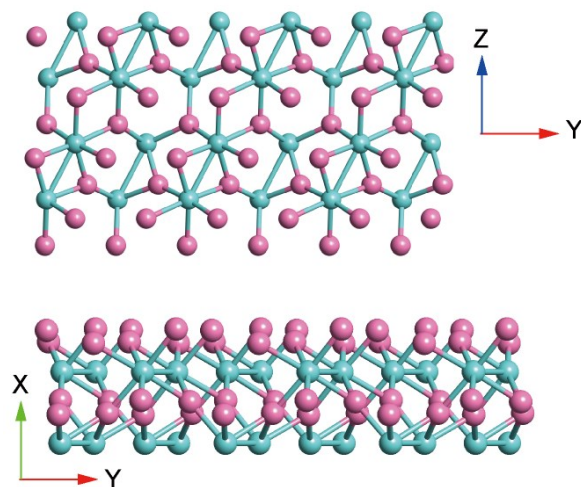


Fig. S1 Crystal structure of MoO_2 . Green and red spheres correspond to Mo and O, respectively.

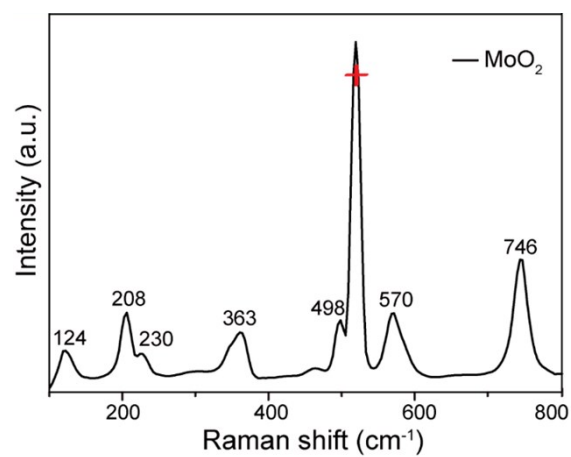


Fig. S2 Raman spectra of the synthesized MoO_2 flakes. The red cross represents the Raman peak of Si.

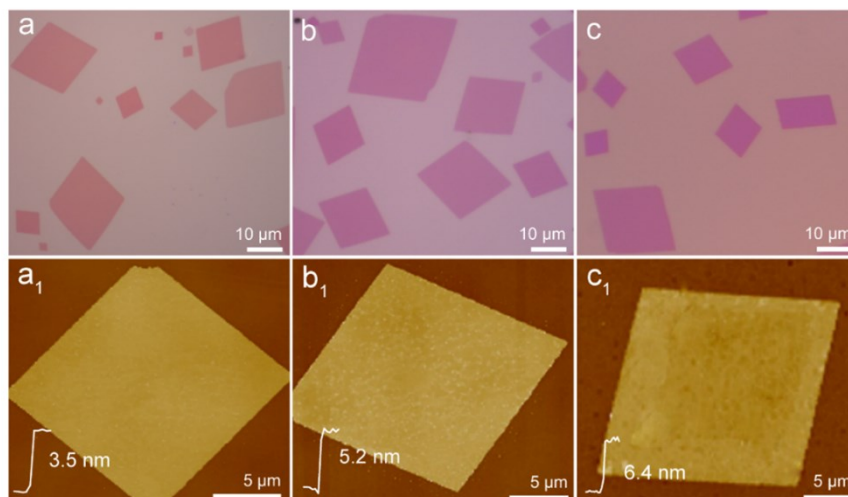


Fig. S3 (a-c) OM images of MoO₂ flakes grown on SiO₂/Si substrate at increasing temperatures of 790°C, 810°C, and 830°C, respectively. (a₁-c₁) AFM height images of the corresponding MoO₂ flakes.

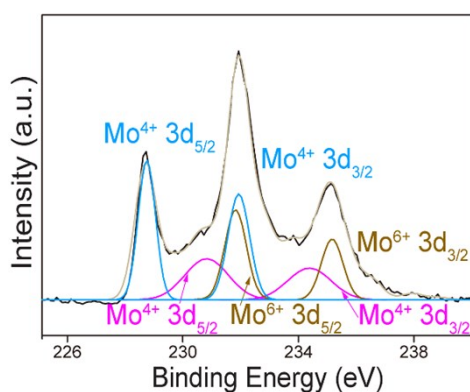


Figure S4. XPS results of Mo 3d regions of the synthesized MoO₂ flakes.

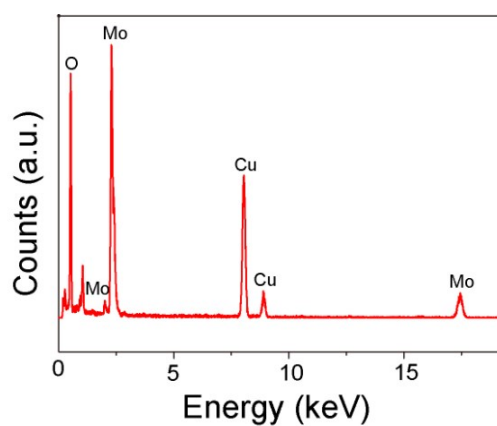


Figure S5. The energy dispersive spectrometry (EDS) analysis of the synthesized MoO₂ flakes.

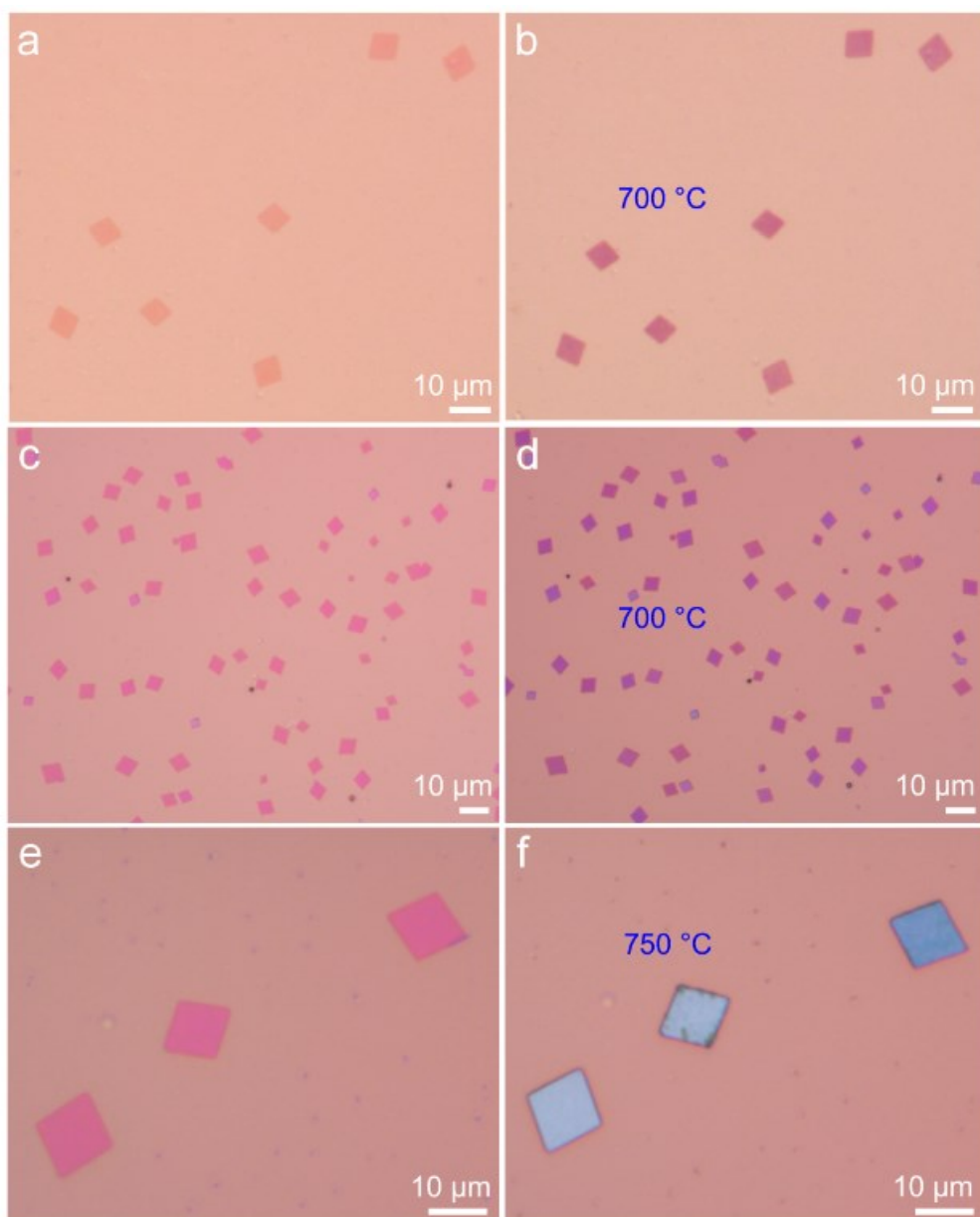


Fig. S6 (a, c, e) OM images of MoO₂ nanosheets. (b, d, f) The corresponding MoN nanosheets synthesized at different temperatures through ammonolysis on the SiO₂/Si substrate.

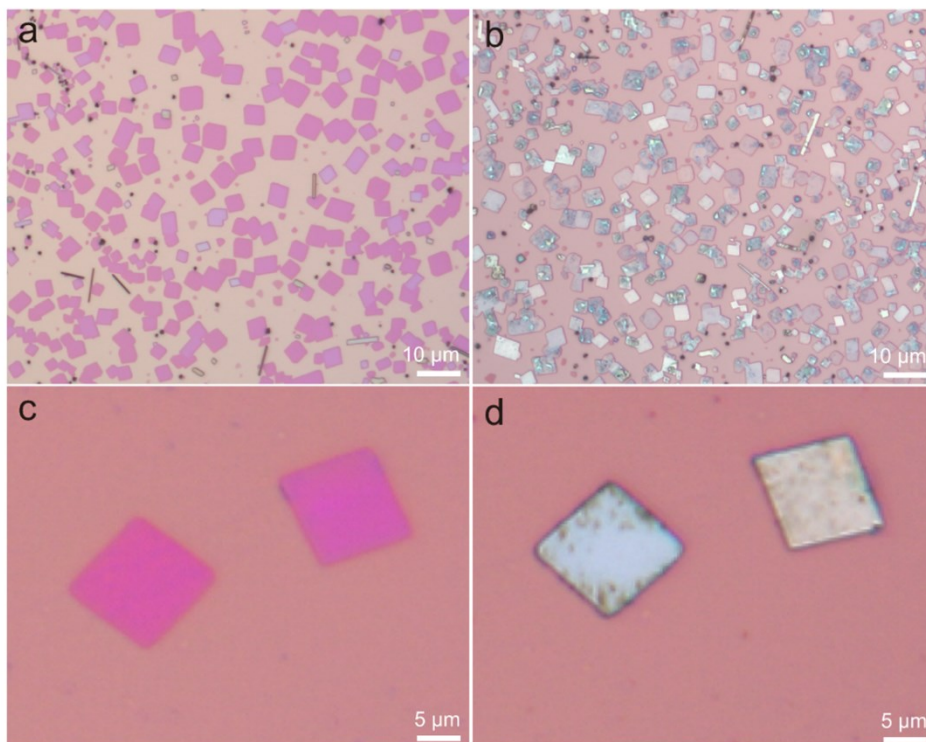


Fig. S7 (a, c) OM images of MoO₂ nanosheets. (b, d) The corresponding MoN nanosheets synthesized at 800 °C through ammonolysis on the SiO₂/Si substrate.

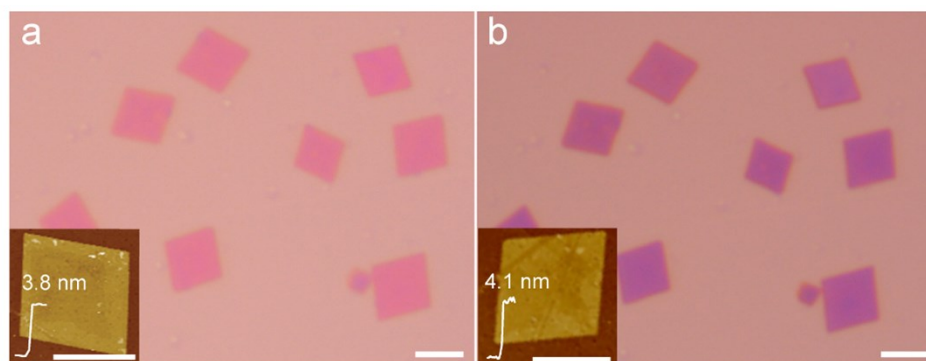


Fig. S8 (a, b) OM images of MoO₂ nanosheets and the corresponding MoN nanosheets on the SiO₂/Si substrate. Inset: AFM height images of the corresponding MoO₂ and the MoN flakes. Scale bars: 10 μm.

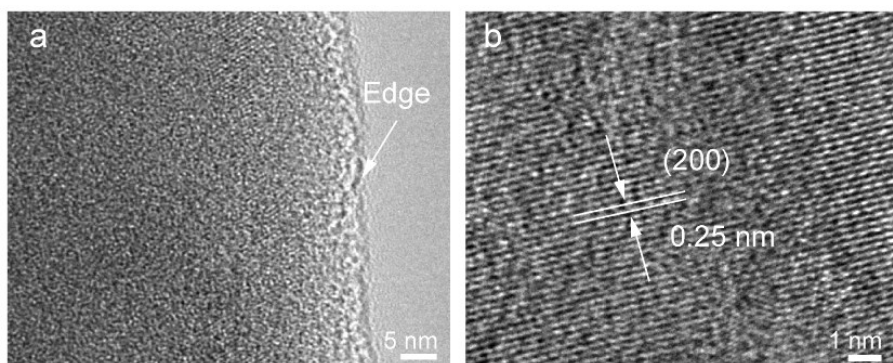


Fig. S9 (a) The HRTEM image of the edge of 2D MoN flake. (b) The HRTEM image of the MoN. (a) Schematic diagram of the electrical contact geometries based on MoN flakes on SiO₂/Si substrate.

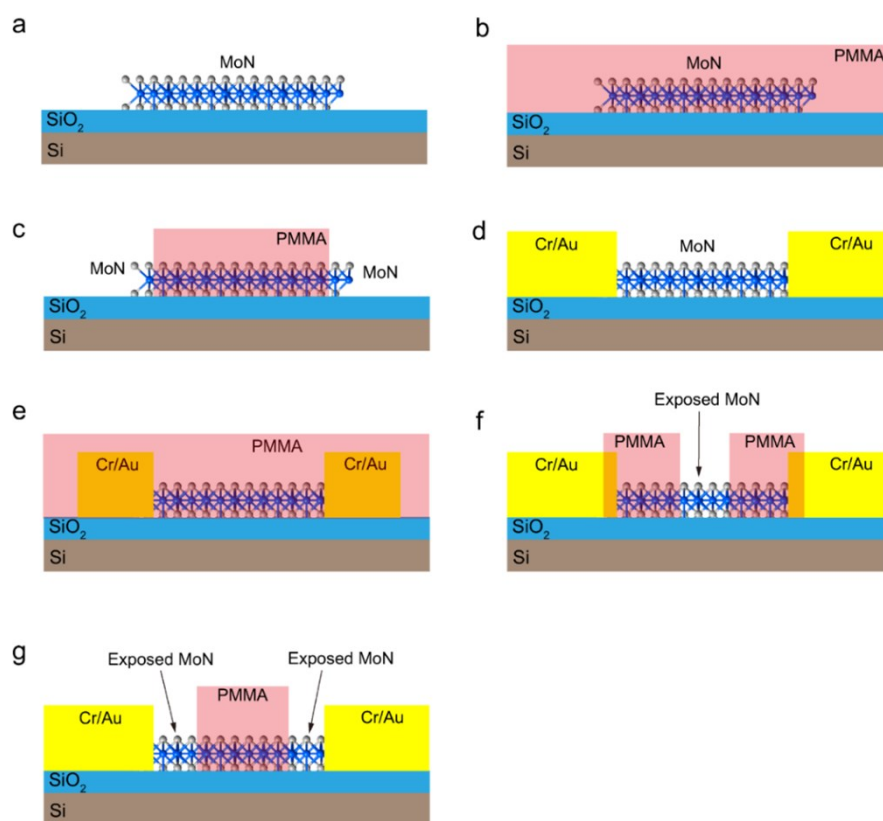


Fig. S10 (a) MoN nanosheets synthesized on SiO₂/Si substrate. (b) SiO₂/Si substrate surface covered with PMMA. (c) Electrode patterns are defined on the PMMA layer. (d) The Cr/Au electrodes are fabricated to contact opened MoN nanosheet part. (e) SiO₂/Si substrate surface covered with PMMA again. (f) Window is opened on the basal plane of MoN. (g) Windows are opened on the edge of MoN.

3. Tables

Table S1. A comparison of the HER parameters of the 2D MoN in this work with various MoN catalysts. (GC: Glass carbon)

Catalysts	Substrate	Electrolytes	η (mV) ($j=10 \text{ mA/cm}^2$)	Tafel Slope (mV/dec)	Active Site	Ref.
MoN	SiO ₂ /Si	1.0 M KOH	248	55.4	Edge	This work
		0.5 M H ₂ SO ₄	322	75.2		
MoN	GC	0.5 M H ₂ SO ₄	~250	76	Grain-boundary	1
MoN	GC	0.1 M perchloric acid.	~410	108	Basal plane and Edge	2
MoN/NF	Ni foam	1.0 M KOH	124	121	Grains	3
		0.5 M H ₂ SO ₄	148	114		
MoN	GC	1.0 M KOH	~400	120.6	Mo site	4
MoN	GC	1.0 M KOH	389	—	Basal plane and Edge	5
		0.5 M H ₂ SO ₄	~410	—		
		Seawater	~500	—		
Dr-MoN	GC	1.0 M KOH	139	61.82	Defect	6
		0.5 M H ₂ SO ₄	125	51.15		

References

1. J. Yan, L. Kong, Y. Ji, Y. Li, J. White, S. Liu, X. Han, S.-T. Lee and T. Ma, *Communications Chemistry*, 2018, **1**.
2. M. Kozejova, V. Latyshev, V. Kavecansky, H. You, S. Vorobiov, A. Kovalcikova and V. Komanicky, *Electrochimica Acta*, 2019, **315**, 9-16.
3. R. Ramesh, D. K. Nandi, T. H. Kim, T. Cheon, J. Oh and S. H. Kim, *ACS Appl Mater Interfaces*, 2019, **11**, 17321-17332.
4. H. Jin, X. Liu, Y. Jiao, A. Vasileff, Y. Zheng and S.-Z. Qiao, *Nano Energy*, 2018, **53**, 690-697.
5. H. Jin, X. Liu, A. Vasileff, Y. Jiao, Y. Zhao, Y. Zheng and S. Z. Qiao, *ACS Nano*,

2018, **12**, 12761-12769.

6. J. Xiong, W. Cai, W. Shi, X. Zhang, J. Li, Z. Yang, L. Feng and H. Cheng, *Journal of Materials Chemistry A*, 2017, **5**, 24193-24198.